

**TRANSIENT THERMOELASTIC PROBLEM FOR
A CIRCULAR SOLID CYLINDER WITH RADIATION**

Dilip B. Kamdi^{1 §}, Namdeo W. Khobragade², Manhor H. Durge³

^{1,2,3}Post Graduate Teaching Department of Mathematics

RTM Nagpur University

Nagpur, 440 033, INDIA

¹e-mail: dilip.kamdi@rediffmail.com

²e-mail: khobragade_nw@rediffmail.com

Abstract: We apply integral transformation techniques to study thermoelastic response of a circular solid cylinder in general, in which sources are generated according to the linear function of the temperature, with boundary conditions of the radiation type. The results are obtained as series of Bessel functions. Numerical calculations are carried out for a particular case of a circular solid cylinder made of aluminum metal and the results are depicted graphically.

AMS Subject Classification: 74J25, 74H99, 74D99

Key Words: transient response, solid cylinder, temperature distribution, thermal stress, integral transform

1. Introduction

As a result of the increased usage of industrial and construction materials the interest in isotropic thermal stress problems has grown considerably. However there are only few studies concerned with the two-dimensional steady state thermal stress. Nowacki [5] has determined steady-state thermal stresses in a thick circular plate subjected to an axisymmetric temperature distribution on the upper face with zero temperature on the lower face and circular edge. Wankhede [9] has determined the quasi-static thermal stresses in circular plate

Received: June 23, 2009

© 2009 Academic Publications

[§]Correspondence address: Plot No. 138, Tajeshwar Nayar, Hudkeshwar Naka, Narasola Road, Nagpur, 440 034, Maharashtra, INDIA

subjected to arbitrary initial temperature on the upper face with lower face at zero temperature. However, there aren't many investigations on transient state. Roy Choudhuri [8] has succeeded in determining the quasi-static thermal stresses in a circular plate subjected to transient temperature along the circumference of circular upper face with lower face at zero temperature and the fixed circular edge thermally insulated. In a recent work, some problems have been solved by Noda et al [6] and Deshmukh et al [1]. In all aforementioned investigations an axisymmetrically heated plate has been considered. Recently, Nasser [4], [1] proposed the concept of heat sources in generalized thermoelasticity and applied to a thick plate problem. He has not however considered any thermoelastic problems with boundary conditions of radiation type, in which sources are generated according to the linear function of the temperatures, which satisfies the time-dependent heat conduction equation. From the previous literatures regarding circular solid cylinder as considered, it was observed by the author that no analytical procedure has been established considering internal heat sources generation within the body.

This paper is concerned with the transient thermoelastic problem in a circular solid cylinder in which sources are generated according to the linear function of temperature, occupying the space $D = \{(x, y, z) \in R^3 : 0 \leq (x^2 + y^2)^{1/2} \leq b, -h \leq z \leq h\}$, where $r = (x^2 + y^2)^{1/2}$ with radiation type boundary conditions.

2. Statement of the Problem

In the first instance, we consider a circular solid cylinder in which sources are generated according to the linear function of temperature. The material is isotropic, homogeneous and all properties are assumed to be constant. Heat conduction with internal heat source and the prescribed boundary conditions of the radiation type are considered. The equation for heat conduction is $\theta(r, z, t)$, the temperature, in cylindrical coordinates is

$$\kappa \left[\frac{1}{r} \frac{\partial}{\partial r} \left(r \frac{\partial \theta}{\partial r} \right) + \frac{\partial^2 \theta}{\partial z^2} \right] + \Theta(r, z, t, \theta) = \frac{\partial \theta}{\partial t}, \quad (1)$$

where $\Theta(r, z, t, \theta)$ is the source function and $\kappa = \lambda/\rho C$, λ being the thermal conductivity of the material, ρ is the density and C is the calorific capacity, assumed to be constant.

For convenience, we consider the undergiven functions as the superposition

of the simpler function [1]

$$\Theta(r, z, t, \theta) = \Phi(r, z, t) + \psi(t) \theta(r, z, t) \tag{2}$$

and

$$\begin{aligned} T(r, z, t) &= \theta(r, z, t) \exp\left[-\int_0^t \psi(\zeta) d\zeta\right], \\ \chi(r, z, t) &= \Phi(r, z, t) \exp\left[-\int_0^t \psi(\zeta) d\zeta\right], \end{aligned} \tag{3}$$

or for the sake of brevity, we consider

$$\chi(r, z, t) = \frac{\delta(r - r_0) \delta(z - z_0)}{2\pi r_0} \exp(-\omega t), \quad 0 \leq r_0 \leq b, \quad -h \leq z_0 \leq h, \quad \omega > 0$$

Substituting equations (2) and (3) in the heat conduction equation (1), one obtains

$$\kappa \left[\frac{1}{r} \frac{\partial}{\partial r} \left(r \frac{\partial T}{\partial r} \right) + \frac{\partial^2 T}{\partial z^2} \right] + \chi(r, z, t) = \frac{\partial T}{\partial t}, \tag{4}$$

where κ is the thermal diffusivity of the material of the cylinder (which is assumed to be constant), subject to the initial and boundary conditions

$$M_t(T, 1, 0, 0) = 0 \quad \text{for all } 0 \leq r \leq b, \quad -h \leq z \leq h, \tag{5}$$

$$M_r(T, 1, 0, b) = 0 \quad \text{for all } -h \leq z \leq h, \quad t > 0, \tag{6}$$

$$\left. \begin{aligned} M_z(T, 1, k_1, h) &= \exp(-\omega t) \delta(r - r_0), \\ M_z(T, 1, k_2, -h) &= \exp(-\omega t) \delta(r - r_0) \end{aligned} \right\} \text{for all } 0 \leq r \leq b, \quad t > 0. \tag{7}$$

The most general expression for these conditions can be given by

$$M_{\vartheta}(f, \bar{k}, \bar{\bar{k}}, \hat{f})_{\vartheta=\vartheta'} = (\bar{k} f + \bar{\bar{k}} \hat{f})_{\vartheta=\vartheta'},$$

where the prime ($\hat{}$) denotes differentiation with respect to ϑ ; $\delta(r - r_0)$ is the Dirac Delta function having $0 \leq r_0 \leq b$; $\omega > 0$ is a constants; $\exp(-\omega t) \delta(r - r_0)$ is the additional sectional heat available on its surface at $z = -h, h$; \bar{k} and $\bar{\bar{k}}$ are radiation constants on the upper and lower surfaces of the cylinder respectively.

The Navier's equations without the body forces for axisymmetric two-dimensional thermoelastic problem can be expressed as (see [6]):

$$\begin{aligned} \nabla^2 u_r - \frac{u_r}{r^2} + \frac{1}{1 - 2\nu} \frac{\partial e}{\partial r} - \frac{2(1 + \nu)}{1 - 2\nu} \alpha_t \frac{\partial \theta}{\partial r} &= 0, \\ \nabla^2 u_z - \frac{1}{1 - 2\nu} \frac{\partial e}{\partial z} - \frac{2(1 + \nu)}{1 - 2\nu} \alpha_t \frac{\partial \theta}{\partial z} &= 0, \end{aligned} \tag{8}$$

where u_r and u_z are the displacement components in the radial and axial directions, respectively and the dilatation e as

$$e = \frac{\partial u_r}{\partial r} + \frac{u_r}{r} + \frac{\partial u_z}{\partial z}.$$

The displacement functions in the cylindrical coordinate system are represented by the Goodier's thermoelastic displacement potential $\phi(r, z, t)$ and Michell's

function M as (see [6]):

$$u_r = \frac{\partial \phi}{\partial r} - \frac{\partial^2 M}{\partial r \partial z}, \quad (9)$$

$$u_z = \frac{\partial \phi}{\partial z} + 2(1 - \nu) \nabla^2 M - \frac{\partial^2 M}{\partial z^2}, \quad (10)$$

in which Goodier's thermoelastic potential must satisfy the equation

$$\nabla^2 \phi = \frac{1 + \nu}{1 - \nu} \alpha_t \theta \quad (11)$$

and the Michell's function M must satisfy the equation

$$\nabla^2(\nabla^2 M) = 0, \quad (12)$$

where

$$\nabla^2 = \frac{1}{r} \frac{\partial}{\partial r} \left(r \frac{\partial}{\partial r} \right) + \frac{\partial^2}{\partial z^2}.$$

The component of the stresses are represented by the use of the potential ϕ and Michell's function M as

$$\sigma_{rr} = 2G \left\{ \left(\frac{\partial^2 \phi}{\partial r^2} - \nabla^2 \phi \right) + \frac{\partial}{\partial z} \left(\nu \nabla^2 M - \frac{\partial^2 M}{\partial r^2} \right) \right\}, \quad (13)$$

$$\sigma_{\theta\theta} = 2G \left\{ \left(\frac{1}{r} \frac{\partial \phi}{\partial r} - \nabla^2 \phi \right) + \frac{\partial}{\partial z} \left(\nu \nabla^2 M - \frac{1}{r} \frac{\partial M}{\partial r} \right) \right\}, \quad (14)$$

$$\sigma_{zz} = 2G \left\{ \left(\frac{\partial^2 \phi}{\partial z^2} - \nabla^2 \phi \right) + \frac{\partial}{\partial z} \left((2 - \nu) \nabla^2 M - \frac{\partial^2 M}{\partial z^2} \right) \right\}, \quad (15)$$

and

$$\sigma_{rz} = 2G \left\{ \frac{\partial^2 \phi}{\partial r \partial z} + \frac{\partial}{\partial r} \left((1 - \nu) \nabla^2 M - \frac{\partial^2 M}{\partial z^2} \right) \right\}, \quad (16)$$

where G and ν are the shear modulus and Poisson's ratio respectively.

The boundary conditions on the traction free surface of a solid cylinder are

$$\sigma_{rr} = \sigma_{rz} = 0 \text{ at } r = b. \quad (17)$$

The equations (1) to (17) constitute the mathematical formulation of the problem under consideration.

3. Solution of the Problem

3.1. Transient Heat Conduction Analysis

In order to solve fundamental differential equation (4) under the boundary condition (6), we firstly introduce the method of Hankel transform [7] of order n over the variable r . Let n be the parameter of the Hankel transform, then the Hankel transform and its inversion theorem are written as

$$g^*(\beta_n, z, t) = \int_0^b g(r, z, t) r k_0(\beta_n, r) dr, \tag{18}$$

$$g(r, z, t) = \sum_{n=1}^{\infty} g^*(\beta_n, z, t) k_0(\beta_n, r),$$

where the symbol (*) means a function in the transformed domain, and the nucleus for the finite Hankel transform defined by

$$k_0(\beta_n, r) = -\frac{\sqrt{2}}{b} \left(\frac{J_0(\beta_n r)}{\beta_n J_1(\beta_n b)} \right).$$

The eigenvalues β_n are the positive roots of the characteristic equation $J_0(\beta b) = 0$, and $J_n(x)$ is the Bessel function of the first kind of order n .

We introduce another integral transform [1] that responds to the boundary conditions of type (7) as

$$\bar{f}(m, t) = \int_{-h}^h f(z, t) P_m(z) dz, \quad f(z, t) = \sum_{m=1}^{\infty} \frac{\bar{f}(m, t)}{\lambda_m} P_m(z), \tag{19}$$

where the symbol (-) means a function in the transformed domain, and the nucleus is given by the orthogonal functions in the interval $-h < z < h$ as

$$P_m(z) = Q_m \cos(a_m z) - W_m \sin(a_m z),$$

$$Q_m = a_m(k_1 + k_2) \cos(a_m h),$$

$$W_m = 2 \cos(a_m h) + (k_2 - k_1) a_m \sin(a_m h),$$

$$\lambda_m = \int_{-h}^h P_m^2(z) dz = h [Q_m^2 + W_m^2] + \frac{\sin(2a_m h)}{2a_m} [Q_m^2 - W_m^2].$$

The eigenvalues a_m are the positive roots of the characteristic equation

$$[k_1 a \cos(ah) + \sin(ah)] [\cos(ah) + k_2 a \sin(ah)]$$

$$= [k_2 a \cos(ah) - \sin(ah)] [\cos(ah) - k_1 a \sin(ah)].$$

Applying the transformation rules (18) and (19) to equation (4) using (6)-(7), one obtains

$$\frac{d\bar{T}^*}{dt} + \kappa E_{m,n} \bar{T}^* = H(\alpha_m, \beta_n), \quad (20)$$

where

$$E_{m,n} = a_m^2 + \beta_n^2$$

and

$$H(\alpha_m, \beta_n) = \left\{ \left[\frac{P_m(h)}{k_1} - \frac{P_m(-h)}{k_2} \right] \kappa r_0 + \frac{P_m(z_0)}{2\pi} \right\} k_0(\beta_n, r_0) e^{-\omega t}.$$

Then, the transformed temperature solution of equation (20) is given by

$$\bar{T}^*(\beta_n, m, t) = \frac{A(n, m)}{\kappa E_{m,n} - \omega} [\exp(-\omega t) - \exp(-\kappa E_{m,n} t)]. \quad (21)$$

Applying the inversion theorems of transformation rules defined in equations (18) and (19) on equation (21) one obtains

$$T(r, z, t) = \sum_{n=1}^{\infty} \sum_{m=1}^{\infty} \wp_{n,m} [\exp(-\omega t) - \exp(-\kappa E_{m,n} t)] P_m(z) k_0(\beta_n, r), \quad (22)$$

where

$$\wp_{n,m} = \frac{A(n, m)}{\lambda_m(\kappa E_{m,n} - \omega)}$$

and

$$A(n, m) = \left\{ \left[\frac{P_m(h)}{k_1} - \frac{P_m(-h)}{k_2} \right] \kappa r_0 + \frac{P_m(z_0)}{2\pi} \right\} k_0(\beta_n, r_0).$$

Taking into account the first equation of equation (3), the temperature distribution is finally represented by

$$\theta(r, z, t) = \sum_{n=1}^{\infty} \sum_{m=1}^{\infty} \wp_{n,m} [\exp(-\omega t) - \exp(-\kappa E_{m,n} t)] P_m(z) k_0(\beta_n, r) \exp\left[\int_0^t \psi(\zeta) d\zeta\right]. \quad (23)$$

The equation (23) represents the temperature at every instant and at all points of a circular cylinder when there are conditions of radiation type.

3.2. Thermoelastic Solution

Referring to the fundamental equation (1) and its solution (23) for the heat conduction problem, the solutions for the displacement function are represented by the Goodier's thermoelastic displacement potential ϕ governed by equation (11) by

$$\phi(r, z, t) = - \left(\frac{1 + \nu}{1 - \nu} \right) a_t \sum_{n=1}^{\infty} \sum_{m=1}^{\infty} \frac{\varrho_{n,m}}{E_{m,n}} [\exp(-\omega t) - \exp(-\kappa E_{m,n} t)] \times P_m(z) k_0(\beta_n, r) \exp\left[\int_0^t \psi(\zeta) d\zeta\right]. \quad (24)$$

Similarly, the solutions for Michell's function M are assumed so as to satisfy the governed condition of equation (12) as

$$M(r, z, t) = - \left(\frac{1 + \nu}{1 - \nu} \right) a_t \sum_{n=1}^{\infty} \sum_{m=1}^{\infty} \frac{\varrho_{n,m}}{E_{m,n}} [\exp(-\omega t) - \exp(-\kappa E_{m,n} t)] \times [A_n J_0(\beta_n r) + C_n(\beta_n r) J_1(\beta_n r)] [\cosh(\beta_n z)] \exp\left[\int_0^t \psi(\zeta) d\zeta\right]. \quad (25)$$

Using (24) and (25) in (9) and (10), one obtains

$$u_r = \left(\frac{1 + \nu}{1 - \nu} \right) a_t \sum_{n=1}^{\infty} \sum_{m=1}^{\infty} \frac{\varrho_{n,m}}{E_{m,n}} [\exp(-\omega t) - \exp(-\kappa E_{m,n} t)] \times \{ \beta_n \sinh(\beta_n z) [A_n(-\beta_n) J_1(\beta_n r) + C_n \beta_n(\beta_n r) J_0(\beta_n r)] - \frac{\sqrt{2}}{b} \frac{J_1(\beta_n r)}{J_1(\beta_n b)} p_m(z) \} \exp\left[\int_0^t \psi(\zeta) d\zeta\right], \quad (26)$$

$$u_z = \left(\frac{1 + \nu}{1 - \nu} \right) a_t \sum_{n=1}^{\infty} \sum_{m=1}^{\infty} \frac{\varrho_{n,m}}{E_{m,n}} [\exp(-\omega t) - \exp(-\kappa E_{m,n} t)] \times \{ a_m [Q_m \sin(a_m z) + W_m \cos(a_m z)] k_0(\beta_n r) + A_n \beta_n^2 (J_0(\beta_n r)) (-3 + 4\nu) [\cosh(\beta_n z)] + C_n \beta_n^2 [4(1 - \nu) J_0(\beta_n r) + (\beta_n r) J_1(\beta_n r) (-3 + 4\nu)] [\cosh(\beta_n z)] \} \times \exp\left[\int_0^t \psi(\zeta) d\zeta\right]. \quad (27)$$

Then, the stress components can be evaluated by substituting the values of thermoelastic displacement potential ϕ from equation (24) and Michell's function

M from equation (25) in equations (13), (14), (15) and (16):

$$\begin{aligned} \sigma_{rr} = & -2G \left(\frac{1+v}{1-v} \right) a_t \sum_{n=1}^{\infty} \sum_{m=1}^{\infty} \frac{\wp_{n,m}}{E_{m,n}} [\exp(-\omega t) - \exp(-\kappa E_{m,n} t)] \\ & \times \left\{ \left[a_m^2 J_0(\beta_n r) - \beta_n \left(\frac{J_1(\beta_n r)}{r} \right) \right] \left(\frac{-\sqrt{2}}{b\beta_n J_1(\beta_n b)} \right) P_m(z) \right. \\ & + \beta_n^3 C_n [(2\nu - 1)J_0(\beta_n r) + (\beta_n r)J_1(\beta_n r)] \sinh(\beta_n z) \\ & \left. + \beta_n^2 A_n \left[\beta_n J_0(\beta_n r) - \frac{J_1(\beta_n r)}{r} \right] \sinh(\beta_n z) \right\} \exp \left[\int_0^t \psi(\zeta) d\zeta \right], \quad (28) \end{aligned}$$

$$\begin{aligned} \sigma_{\theta\theta} = & -2G \left(\frac{1+v}{1-v} \right) a_t \sum_{n=1}^{\infty} \sum_{m=1}^{\infty} \frac{\wp_{n,m}}{E_{m,n}} [\exp(-\omega t) - \exp(-\kappa E_{m,n} t)] \\ & \times \left\{ \left[\beta_n \left(\frac{J_1(\beta_n r)}{r} \right) - E_{m,n} J_0(\beta_n r) \right] \left(\frac{\sqrt{2}}{b\beta_n J_1(\beta_n b)} \right) P_m(z) \right. \\ & + \beta_n^2 A_n \left(\frac{J_1(\beta_n r)}{r} \right) \sinh(\beta_n z) \\ & \left. + \beta_n^3 C_n (2\nu - 1) J_0(\beta_n r) \sinh(\beta_n z) \right\} \exp \left[\int_0^t \psi(\zeta) d\zeta \right], \quad (29) \end{aligned}$$

$$\begin{aligned} \sigma_{zz} = & -2G \left(\frac{1+v}{1-v} \right) a_t \sum_{n=1}^{\infty} \sum_{m=1}^{\infty} \frac{\wp_{n,m}}{E_{m,n}} [\exp(-\omega t) - \exp(-\kappa E_{m,n} t)] \\ & \times \left\{ \frac{-\sqrt{2}}{b} \left(\frac{\beta_n J_0(\beta_n r)}{J_1(\beta_n b)} \right) P_m(z) - \beta_n^3 A_n J_0(\beta_n r) \sinh(\beta_n z) \right. \\ & + \beta_n^3 C_n [2(2 - \nu)J_0(\beta_n r) - (\beta_n r)J_1(\beta_n r)] \sinh(\beta_n z) \left. \right\} \\ & \times \exp \left[\int_0^t \psi(\zeta) d\zeta \right], \quad (30) \end{aligned}$$

and

$$\begin{aligned} \sigma_{rz} = & -2G \left(\frac{1+v}{1-v} \right) a_t \sum_{n=1}^{\infty} \sum_{m=1}^{\infty} \frac{\wp_{n,m}}{E_{m,n}} [\exp(-\omega t) - \exp(-\kappa E_{m,n} t)] \\ & \times \left\{ -a_m [W_m \cos(a_m z) + Q_m \sin(a_m z)] \frac{\sqrt{2}}{b} \left(\frac{J_1(\beta_n r)}{J_1(\beta_n b)} \right) \right. \end{aligned}$$

$$\begin{aligned}
 & +\beta_n^3 A_n J_1(\beta_n r) \cosh(\beta_n z) - \beta_n^3 C_n [2(1 - \nu) J_1(\beta_n r) \\
 & + (\beta_n r) J_0(\beta_n r)] \cosh(\beta_n z) \} \exp\left[\int_0^t \psi(\zeta) d\zeta\right]. \quad (31)
 \end{aligned}$$

3.3. Determination of Unknown Arbitrary Function A_n and C_n

Applying boundary condition (17) to the equation (28) and (31) one obtains

$$A_n = \sum_{n=1}^{\infty} \sum_{m=1}^{\infty} \frac{\sqrt{2}\{\cosh(\beta_n z) P_m(z) [J_0(\beta_n b) (\bar{X} + \bar{Y}) + \lambda] + \delta \sinh(\beta_n z) \gamma\}}{\beta_n^4 b \sinh(\beta_n z) \cosh(\beta_n z) \{J_0(\beta_n b) [M + N]\}}$$

and

$$\begin{aligned}
 C_n = & \sum_{n=1}^{\infty} \sum_{m=1}^{\infty} \frac{\sqrt{2}\{\cosh(\beta_n z) P_m(z) [a_m^2 J_0(\beta_n b) - \left(\frac{\beta_n}{b}\right) J_1(\beta_n b)] + \delta \sinh(\beta_n z) \eta\}}{\beta_n^3 b \sinh(\beta_n z) \cosh(\beta_n z) \{(\beta_n b) \beta_n [J_0(\beta_n b)]^2 + [J_1(\beta_n b)]^2 [\beta_n^2 - 2\left(\frac{1-\nu}{b}\right)]\}},
 \end{aligned}$$

where

$$\begin{aligned}
 \bar{X} &= 2(1 - \nu) a_m^2 - \beta_n (\beta_n b), & \bar{Y} &= \frac{a_m^2 (\beta_n b)}{J_1(\beta_n b)}, \\
 \lambda &= 2(1 - \nu) \beta_n J_1(\beta_n b), & \delta &= a_m [W_m \cos(a_m z) + Q_m \sin(a_m z)], \\
 \gamma &= (2\nu - 1) J_0(\beta_n b) + \beta_n b J_1(\beta_n b), & \eta &= \frac{J_1(\beta_n b)}{b} - \beta_n J_0(\beta_n b), \\
 M &= (1 - \beta_n^2) J_1(\beta_n b) + (\beta_n b) J_0(\beta_n b), & N &= [J_1(\beta_n b)]^2 [\beta_n (b) - 2(1 - \nu) b^{-1}].
 \end{aligned}$$

3.4. Special Case

Set

$$\psi(\zeta) = \zeta. \quad (32)$$

Using (32) into equation (23), (26), (27) and (28) to (31) one obtains the expressions for temperature distribution displacement and stresses respectively as follows:

$$\begin{aligned}
 \theta(r, z, t) = & \sum_{n=1}^{\infty} \sum_{m=1}^{\infty} \wp_{n,m} [\exp(-\omega t) - \exp(-\kappa E_{m,n} t)] P_m(z) k_0(\beta_n, r) \exp(t^2/2), \quad (33)
 \end{aligned}$$

$$\begin{aligned}
u_r = & \left(\frac{1+v}{1-v} \right) a_t \sum_{n=1}^{\infty} \sum_{m=1}^{\infty} \frac{\wp_{n,m}}{E_{m,n}} [\exp(-\omega t) - \exp(-\kappa E_{m,n} t)] \\
& \times \{ \beta_n \sinh(\beta_n z) [A_n(-\beta_n) J_1(\beta_n r) + C_n \beta_n (\beta_n r) J_0(\beta_n r)] \\
& \quad - \frac{\sqrt{2}}{b} \frac{J_1(\beta_n r)}{J_1(\beta_n b)} P_m(z) \} \exp(t^2/2), \quad (34)
\end{aligned}$$

$$\begin{aligned}
u_z = & \left(\frac{1+v}{1-v} \right) a_t \sum_{n=1}^{\infty} \sum_{m=1}^{\infty} \frac{\wp_{n,m}}{E_{m,n}} [\exp(-\omega t) - \exp(-\kappa E_{m,n} t)] \\
& \times \{ a_m [Q_m \sin(a_m z) + W_m \cos(a_m z)] k_0(\beta_n r) \\
& + A_n \beta_n^2 (J_0(\beta_n r)) (-3 + 4\nu) \cosh(\beta_n z) \\
& + C_n \beta_n^2 [4(1-\nu) J_0(\beta_n r) \\
& \quad + (\beta_n r) J_1(\beta_n r) (-3 + 4\nu)] \cosh(\beta_n z) \} \exp(t^2/2), \quad (35)
\end{aligned}$$

$$\begin{aligned}
\sigma_{rr} = & -2G \left(\frac{1+v}{1-v} \right) a_t \sum_{n=1}^{\infty} \sum_{m=1}^{\infty} \frac{\wp_{n,m}}{E_{m,n}} [\exp(-\omega t) - \exp(-\kappa E_{m,n} t)] \\
& \times \left\{ \left[a_m^2 J_0(\beta_n r) - \beta_n \left(\frac{J_1(\beta_n r)}{r} \right) \right] \left(\frac{-\sqrt{2}}{b \beta_n J_1(\beta_n b)} \right) P_m(z) \right. \\
& + \beta_n^2 A_n \left[\beta_n J_0(\beta_n r) - \frac{J_1(\beta_n r)}{r} \right] \sinh(\beta_n z) \\
& \left. + \beta_n^3 C_n [(2\nu - 1) J_0(\beta_n r) + (\beta_n r) J_1(\beta_n r)] \sinh(\beta_n z) \right\} \exp(t^2/2), \quad (36)
\end{aligned}$$

$$\begin{aligned}
\sigma_{\theta\theta} = & -2G \left(\frac{1+v}{1-v} \right) a_t \sum_{n=1}^{\infty} \sum_{m=1}^{\infty} \frac{\wp_{n,m}}{E_{m,n}} [\exp(-\omega t) - \exp(-\kappa E_{m,n} t)] \\
& \times \left\{ \left[\beta_n \left(\frac{J_1(\beta_n r)}{r} \right) - E_{m,n} J_0(\beta_n r) \right] \left(\frac{\sqrt{2}}{b \beta_n J_1(\beta_n b)} \right) P_m(z) \right. \\
& \left. + \beta_n^2 A_n \left(\frac{J_1(\beta_n r)}{r} \right) \sinh(\beta_n z) + \beta_n^3 C_n (2\nu - 1) J_0(\beta_n r) \sinh(\beta_n z) \right\} \\
& \times \exp(t^2/2), \quad (37)
\end{aligned}$$

$$\begin{aligned}
\sigma_{zz} = & -2G \left(\frac{1+v}{1-v} \right) a_t \sum_{n=1}^{\infty} \sum_{m=1}^{\infty} \frac{\wp_{n,m}}{E_{m,n}} [\exp(-\omega t) - \exp(-\kappa E_{m,n} t)] \\
& \times \left\{ \frac{-\sqrt{2}}{b} \frac{\beta_n J_0(\beta_n r)}{J_1(\beta_n b)} \times P_m(z) - \beta_n^3 A_n J_0(\beta_n r) \sinh(\beta_n z) \right\}
\end{aligned}$$

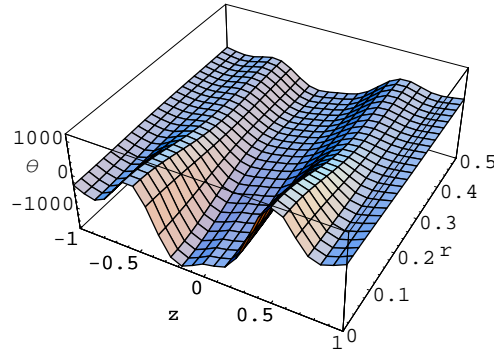


Figure 1: Temperature distribution along r - and z -direction for $t = 3$

$$\begin{aligned}
 &+ \beta_n^3 C_n [2(2 - \nu)J_0(\beta_n r) - (\beta_n r)J_1(\beta_n r)] \sinh(\beta_n z) \} \\
 & \hspace{20em} \times \exp(t^2/2), \tag{38}
 \end{aligned}$$

$$\begin{aligned}
 \sigma_{rz} = & -2G \left(\frac{1 + \nu}{1 - \nu} \right) a_t \sum_{n=1}^{\infty} \sum_{m=1}^{\infty} \frac{\wp_{n,m}}{E_{m,n}} [\exp(-\omega t) - \exp(-\kappa E_{m,n} t)] \\
 & \times \left\{ -a_m [W_m \cos(a_m z) + Q_m \sin(a_m z)] \frac{\sqrt{2}}{b} \left(\frac{J_1(\beta_n r)}{J_1(\beta_n b)} \right) \right. \\
 & \quad + \beta_n^3 A_n J_1(\beta_n r) \cosh(\beta_n z) \\
 & \quad \left. - \beta_n^3 C_n [2(1 - \nu)J_1(\beta_n r) + (\beta_n r)J_0(\beta_n r)] \cosh(\beta_n z) \right\} \\
 & \hspace{20em} \times \exp(t^2/2). \tag{39}
 \end{aligned}$$

4. Numerical Results, Discussion and Remarks

To interpret the numerical computations, we consider material properties of Aluminum metal, which can be commonly used in both, wrought and cast forms. The low density of aluminum results in its extensive use in the aerospace industry, and in other transportation fields. Its resistance to corrosion leads to its use in food and chemical handling (cookware, pressure vessels, etc.) and to architectural uses.

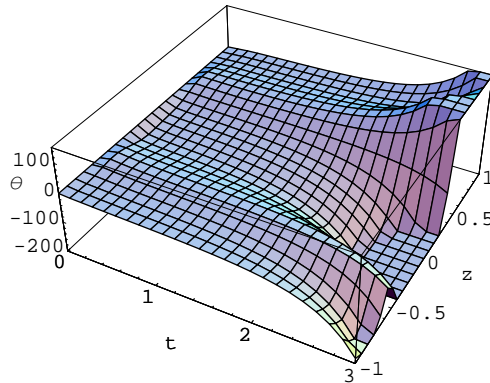


Figure 2: Temperature distribution along z -direction with varying time for $r = 0.5$

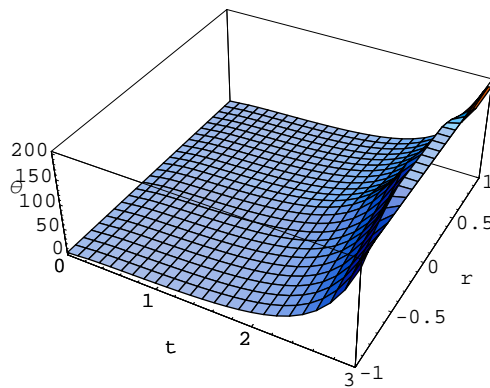


Figure 3: Temperature distribution along r -direction with varying time for $z = 1$

In the foregoing analysis are performed by setting the radiation coefficients constants, $k_1 = k_2 = 0.86$ so as to obtain considerable mathematical simplicities. The other parameters considered are $r_0 = 0.20$, $z_0 = 0.5$ and $\omega = 0.5$. The derived numerical results from equations (22) and (34) to (41) have been illustrated graphically with internal heat source and with available additional sectional heat on its flat surface at $z = 1$.

Figure 1 shows the temperature distribution along the radial and thickness direction of the circular cylinder at $t = 3$. It is observed that due to the thickness

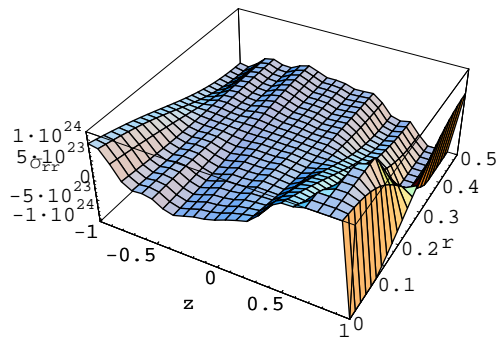


Figure 4: Radial stress distribution along r - and z -direction for $t = 3$

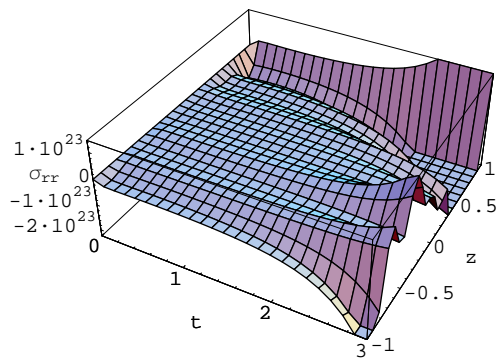


Figure 5: Radial stress distribution along z -direction with varying time for $r = 0.5$

of the cylinder, a steep increase in temperature was found at the beginning of the transient period. As expected, temperature drop becomes more and more gradually along the central portion of thickness direction. Finally temperature distribution further increase and attains zero value at the extreme end. Figure 2 and Figure 3 show the temperature distribution with vary time function along z -direction and r -direction and increased temperature trend is observed at $z = 1$ where we have provided additional sectional heat supply on its flat surface, whereas with increase in time temperature distribution gradually increase from

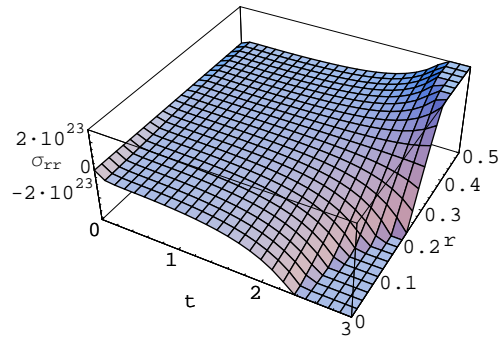


Figure 6: Radial stress distribution along r -direction with varying time for $z = 1$

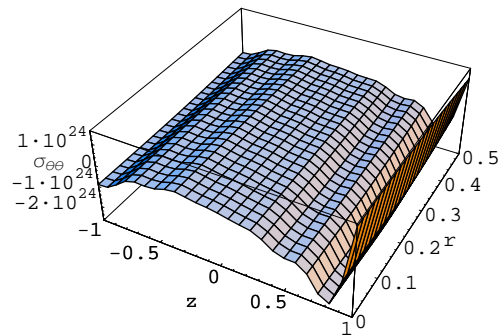


Figure 7: Tangential stress distribution along r - and z -direction for $t = 3$

the center of core to the outer edge.

Figure 4 and Figure 5 show the radial stress distribution σ_{rr} along the radial and thickness direction of the circular solid cylinder and z -direction with varying time. From the figure, the location of points of minimum stress occurs at the end points through-the-thickness direction, while the thermal stress response are maximum at the inner surface leading inner part being under tensile stress. Figure 6 shows the radial stress distribution σ_{rr} along the radial direction of the solid cylinder with varying time. It is observed that stress at the outer

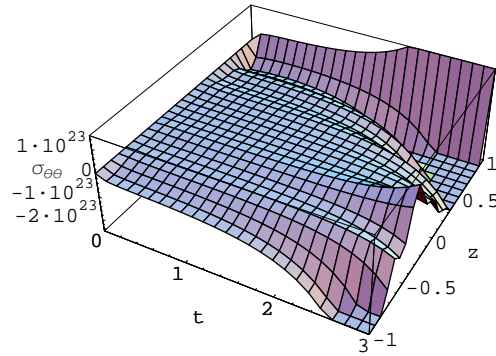


Figure 8: Tangential stress distribution along z -direction with varying time for $r = 0.5$

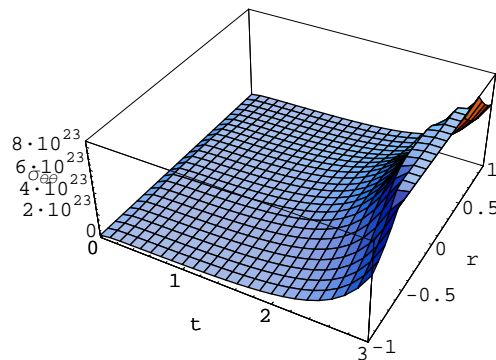


Figure 9: Tangential stress distribution along r -direction with varying time for $t = 3$

extreme end is high and it gradually decreases towards the center core till it approaches zero.

Figure 7 shows the tangential stress distribution $\sigma_{\theta\theta}$ along the radial and thickness direction of the circular solid cylinder at $t = 3$. Figure 8 shows the stress distribution along r -direction with varying time. The tangential stress follows a sinusoidal nature with high crest and troughs at both end. Figure 9 shows the tangential stress distribution along the thickness direction of the solid cylinder with varying time. It is observed that stress gradually increases

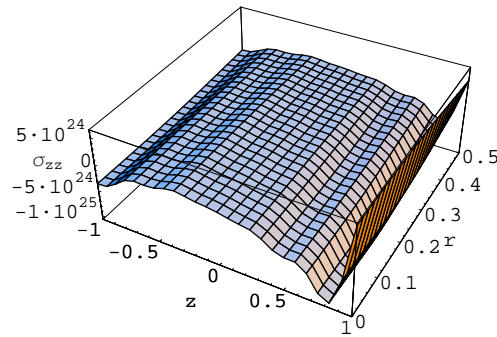


Figure 10: Axial stress distribution along r - and z -direction for $t = 3$

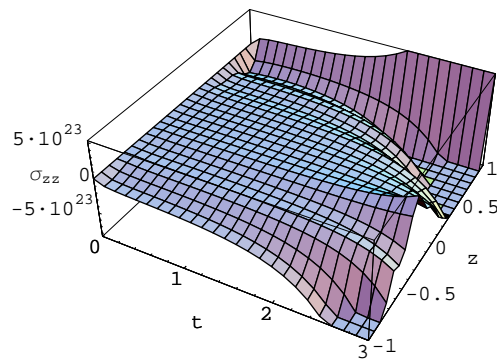


Figure 11: Axial stress distribution along z -direction with varying time for $r = 0.5$

with time.

Figure 10, Figure 11 and Figure 12 shows the axial stress distribution σ_{zz} , which is similar in nature, but higher in magnitude as compared to tangential stress component.

Figure 13 and Figure 14 show the shear stress distribution σ_{rz} along the radial and thickness direction of the solid cylinder at $t = 3$ and z -direction with varying time function. A steep change in stress was found may be due to the thickness of the cylinder. The shear stress also follows more sine waveform with

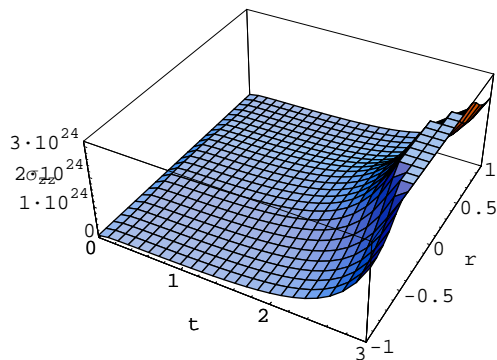


Figure 12: Axial stress distribution along r -direction with varying time for $t = 3$

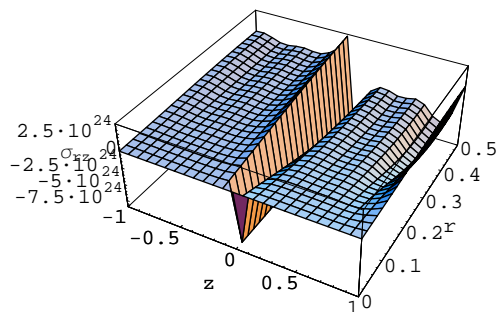


Figure 13: Shear stress distribution along r - and z -direction for $t = 3$

high peaks and troughs along the thickness direction. Figure 15 shows the shear stress distribution along the radial direction of the solid cylinder with varying time. It is observed that stress gradually increases with time and is highest at the outer edge.

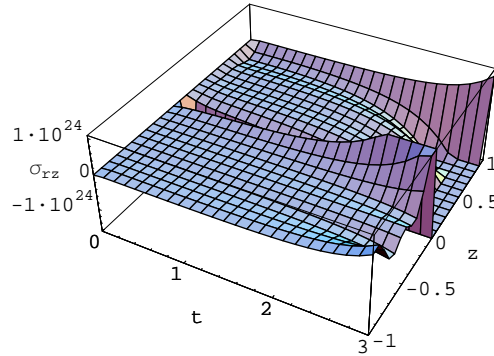


Figure 14: Shear stress distribution along z -direction with varying time for $r = 0.5$

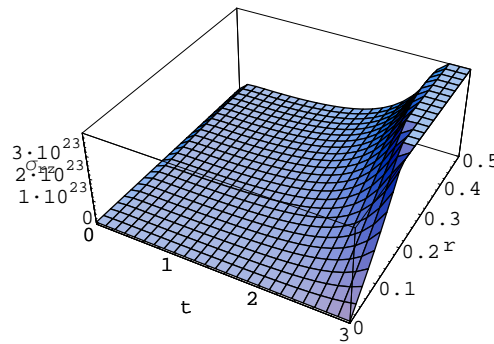


Figure 15: Shear stress distribution along r -direction with varying time for $t = 3$

5. Conclusion

In this problem, the temperature distributions, displacement and stress functions at the edge $z = h$ of a circular cylinder in which sources are generated according to the linear function of the temperature have been obtained where the cylinder is subjected to known heat source function $\exp(-\omega t)\delta(r - r_0)$. As a particular case mathematical model is constructed for $\psi(\zeta) = \zeta$ and performed numerical calculations. We develop the analysis for the temperature

| | |
|--|-----------------------|
| Modulus of Elasticity, E (dynes/cm ²) | 6.9×10^{11} |
| Shear modulus, G (dynes/cm ²) | 2.7×10^{11} |
| Poisson ratio, ν | 0.281 |
| Thermal expansion coefficient, α_t (cm/cm- ⁰ C) | 25.5×10^{-6} |
| Thermal diffusivity, κ (cm ² /sec) | 0.86 |
| Thermal conductivity, λ (cal-cm/ ⁰ C/sec/ cm ²) | 0.48 |
| Outer radius, b (cm) | 0.5 |
| Thickness, h (cm) | 1 |

Table 1: Material properties and parameters used in this study property values are nominal

field by introducing the transformation techniques. Assigning suitable values to the parameters and functions in the equations of temperature, displacements and stresses respectively, expressions of special interest can be derived for any particular case of special interest.

Acknowledgements

The authors are thankful to University Grant Commission, New Delhi for providing the partial financial assistance under major research project scheme.

References

- [1] V.S. Kulkarni, K.C. Deshmukh, Quasi-static thermal stresses in a thick circular plate, *Appl. Math. Mod.*, **31** (2007), 1479-1488.
- [2] E. Marchi, A. Fasulo, Heat conduction in sectors of hollow cylinder with radiation, *Atti. della Acc. delle Sci. di Torino*, **1** (1967), 373-382.
- [3] M. El-Maghraby Nasser, Two dimensional problems with heat sources in generalized thermoelasticity, *J. Therm. Stresses*, **27** (2004), 227-239.
- [4] M. El-Maghraby Nasser, Two dimensional problems for a thick plate with heat sources in generalized thermoelasticity, *J. Therm. Stresses*, **28** (2005), 1227-1241.

- [5] W. Nowacki, The state of stress in a thick circular plate due to temperature field, *Bull. Sci. Acad. Polon Sci. Tech.*, **5** (1957), 227.
- [6] Naotake Noda, Richard B. Hetnarski, Yashinobu Tanigawa, *Thermal Stresses*, Second Edition, Taylor and Francis, New York (2003), 260.
- [7] M. Necati Ozisik, *Boundary Value Problems of Heat Conductions*, International Text Book Company, Scranton, Pennsylvania (1986), 135.
- [8] S.K. Roy Choudhary, A note on quasi-static thermal deflection of a thin clamped circular plate due to ramp-type heating of a concentric circular region of the upper face, *J. of the Franklin Institute*, **206** (1973), 213-219.
- [9] P.C. Wankhede, On the quasi-static thermal stresses in a circular plate, *Indian J. Pure Appl. Math.*, **13**, No. 11 (1982), 1273-1277.